HHS Public Access

Author manuscript

Bioorg Chem. Author manuscript; available in PMC 2025 October 16.

Published in final edited form as:

Bioorg Chem. 2025 January ; 154: 108039. doi:10.1016/j.bioorg.2024.108039.

Enzyme fragment complementation driven by nucleic acid hybridization sans self-labeling protein

Zihan Xu,

Xiaoyu Zhang,

Chandan Pal,

Eriks Rozners,

Brian P. Callahan*

Department of Chemistry, Binghamton University, The State University of New York, 4400 Vestal Parkway East Binghamton, New York 13902, USA

Abstract

A modified enzyme fragment complementation assay has been designed and validated as a turn-on biosensor for nucleic acid detection in dilute aqueous solution. The assay is target sequence-agonistic and uses fragments of NanoBiT, the split luciferase reporter enzyme, that are esterified enzymatically at their C-termini to steramers, sterol-linked oligonucleotides. The *Drosophila* hedgehog autoprocessing domain, DHhC, serves as the self-cleaving enzyme for the NanoBiT-steramer bioconjugations. Unlike current approaches, the final bioconjugate generated by DHhC and used for nucleic acid detection is free of self-labeling passenger protein. In the presence of single stranded (ss) DNA or RNA template with adjacent segments complementary to the Nano-BiT steramer oligonucleotides, the two NanoBiT fragments associate productively, reconstituting NanoBiT's luciferase activity. In samples containing ssDNA or RNA template at low nM concentrations, NanoBiT luminescence exceeded background signal by 30- to 60-fold. The steramer probe sequences used to prepare these sensors are unconstrained in length and composition. In the absence of sequence constraints of the probe element and without the added bulk of a self-labeling protein, these NanoBiT-steramer bioconjugates open new applications in the programmable detection of small fragments of coding and noncoding DNA and RNA.

1. Introduction

Proteins whose function can be turned on or off experimentally enable biosensing applications and provide valuable reagents to probe complex biological pathways.

*Corresponding author. callahan@binghamton.edu (B.P. Callahan).

CRediT authorship contribution statement

Zihan Xu: Writing – review & editing, Methodology, Investigation, Formal analysis, Data curation. **Xiaoyu Zhang:** Methodology. **Chandan Pal:** Writing – review & editing, Methodology. **Eriks Rozners:** Writing – review & editing, Methodology. **Brian P. Callahan:** Writing – review & editing, Writing – original draft, Project administration, Funding acquisition, Conceptualization.

Declaration of competing interest

The authors declare the following financial interests/personal relationships which may be considered as potential competing interests: Brian Callahan has patent #US 10,738,338 B2 issued to SUNY Research Foundation of New York. Brian Callahan has patent #U.S. 12,077,795 issued to SUNY Research Foundation of New York. If there are other authors, they declare that they have no known competing financial interests or personal relationships that could have appeared to influence the work reported in this paper.

Temperature sensitive phenotypes, for example, are possible with destabilized mutant proteins that aggregate or fail to fold above some threshold temperature [1]. Domain insertion into a protein with ligand binding modules [2], light responsive polypeptides, such as LOV2, or light responsive prosthetic groups, like azobenzene, provide alternative and potentially reversible means for controlling protein function [3–6].

Protein fragment complementation, the focus of the present work, may be the most widely applied approach to achieve conditional activity [7,8]. The protein of interest is "split" into non-functional, weakly interacting fragments. Under selected conditions, those fragments are driven to assemble into a functional heterodimeric complex [9–11]. Enzymatic and nonenzymatic proteins are amenable to this type of manipulation [12]. Different triggers have been used to promote fragment complementation, such as noncovalent interactions of fused partner proteins [13,14], proteolytic cleavage [15], as well as by chemical dimerizers for concentration-responsive complementation [8,16].

Here we explore nucleic acid hybridization as a driver of enzyme fragment complementation with a view toward fundamental and applied uses in RNA and DNA biosensing [17–21]. As depicted in Scheme 1, we pursued a split reporter enzyme where the two polypeptide fragments were covalently linked to single-stranded oligonucleotides. The sequences of those oligos would be designed for hybridization at adjacent sites on a DNA or RNA of interest. In this prototype biosensor, enzyme activity is the proxy for (complementary) nucleic acid.

2. Results and discussion

We selected the split reporter enzyme, NanoBiT, derived by Wood and colleagues from the bioluminescent nanoluciferase, and comprised of a large (LrgBiT, 18 kDa) and a small (SmBiT, 1.2 kDa) fragment [22]. Intrinsic affinity of LrgBiT and SmBiT is weak (K_D ~ 100–200 μM), reducing spontaneous association. When LrgBiT and SmBiT are induced to associate productively, the two fragments reconstitute functional NanoBiT as an engineered heterodimer. Enzymatic oxidation of coelenterazine or its synthetic analog furimazine by NanoBiT generates glow-type luminescence. Like nanoluciferase, NanoBiT activity is independent of ATP and cofactor/coenzymes, which simplifies experimental design. Other advantages of luciferase reporters include the absence of background signal in most biological samples and their robust output luminescence, permitting qualitative yes/no analysis even with cellphone-based imaging devices [20,23,24].

To attach oligodeoxynucleotides site-specifically to LrgBiT and SmBiT with 1:1 stoichiometry we used the enzymatic autoprocessing domain found in *Drosophila* hedgehog protein, hereafter, DHhC [25]. The native function of DHhC is to cleave off and covalently attach cholesterol to an adjacent *N*-terminal polypeptide within a precursor polypeptide [26,27]. We and others have found that DHhC is substrate indiscriminate, retaining activity when fused to heterologous *N*-terminal polypeptides (e.g., nanoluciferase, maltose binding protein, lysozyme, cyan fluorescent protein, etc.) and accepting a broad range of cholesterol analogs as alternative substrates, including monosterylated oligonucleotides we call steramers [25,27,28]. In a steramer, depicted below, the sterol's fused ring structure

is maintained for substrate recognition by DHhC while the isooctyl sterol side chain is modified to serve as a linker for covalent oligo attachment. DHhC is active toward steramer substrates with oligos of varying sequence, length, chemical modification and secondary structure [25]. We recently reported a scalable means for preparing steramers by using solid phase synthesis [29].

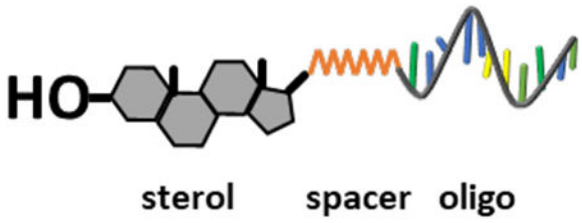

The general method for 1:1 protein of interest (POI)-steramer bioconjugation using DHhC resembles that of other self-labeling proteins such as HaloTag, and HUH tag [30,31]. However, the key distinction is that DHhC self-cleaves from the bioconjugate product simultaneously with the POI-steramer coupling. Self-labeling domains, by contrast, must remain attached to the product as extraneous bulk (Fig. 1).

A chimeric gene construct is assembled first in which the POI is fused at its C-terminus to DHhC. A single glycine residue represents the minimal spacer between the POI and the first residue of DHhC. Here, we incorporated a longer Gly-Ser-Gly spacer for flexibility in split NanoBiT reassembly [22,32,33]. DHhC is activated for bioconjugation of the POI by addition of steramer. No ATP or cofactors are involved.

The chemi-enzymatic approach to generate the two NanoBiT steramer components by DHhC is summarized in Fig. 2. For the NanoBiT components, we designed constructs where LrgBiT and SmBiT were fused to an *N*-terminal SUMO tag as a solubility enhancer [34]. A C-terminal His_6 tag was added to DHhC for precursor purification. The two constructs, SUMO-LrgBiT-DHhC-His_6 and SUMO-SmBiT-DHhC-His_6, were overexpressed in *E. coli* in soluble form and purified under native conditions by Ni-NTA chromatography (Supporting Fig. 1).

For pilot studies, oligo sequences for two steramers were designed for annealing at adjacent sites within the NSP10 gene from SARS-CoV-2 (Table 1). NSP10 encodes a protein cofactor of the viral 2′-O-RNA methyltransferase [35,36]. Unlike variability reported in other SARS-CoV-2 coding sequences, NSP10 appears relatively stable [37,38], making this region an attractive target for molecular detection.

Steramers were prepared in two steps: first, joining heptanediamine to 23,24-bisnor-5-cholenic acid-3β-ol to produce **III**, followed by amide coupling of **III** to resin-bound oligodeoxynucleotide equipped with 5′ NHS ester modification (Fig. 2). After deprotection and resin cleavage, the two steramers, S1 and S2, were desalted and isolated by reverse phase chromatography followed by MS analysis (Supporting information).

Progress of covalent steramer attachment by DHhC to the NanoBiT fragments was monitored by denaturing SDS-PAGE with staining by Gel-Red (nucleic acid specific) and

Coomassie blue. In a typical experiment, reactions were initiated on the benchtop at 23 °C in Bis-Tris buffered DHhC assay solution (pH 7.1) containing 1.5 μM precursor protein and 50 μM steramer. Initial steramer concentration represents 2x the K_M value with DHhC, determined separately using a FRET-based DHhC activity assay (Supporting Fig. 2) [28]. Analysis of the reaction mixture by denaturing SDS-PAGE showed the consumption of precursor protein along with the accumulation of the respective bioconjugate. Fig. 2, right side, is a representative gel for the SUMO-LrgBiT coupling to steramer, S2, catalyzed by DHhC. The calculated molecular weight is 36.6 kDa for the product, which agrees well with the extrapolated value of 37.1 kDa, based on comparison to the MW ladder. This species is visible with Coomassie staining and the nucleic acid stain, Gel-Red. Only trace amounts of the hydrolytic unconjugated side-product, SUMO-LrgBiT, was observed (Fig. 2, see gel, “h”). Reactions ranged from 50-80 % conversion, with highest yields coming from precursor protein that was isolated by Ni-NTA chromatography then further purified by *SEC*. Agarose gel extraction offered a convenient and inexpensive means for final isolation of the NanoBiT-steramer bioconjugates (Supporting Fig. 3).

Robust luminescence signal from reconstituted NanoBiT was observed when the two bioconjugates, hereafter ^{SUMO}Sm-S1 and ^{SUMO}Lg-S2, were combined with a complementary single stranded NSP10 oligodeoxynucleotide template, d-NSP10 (Fig. 3A). NanoBiT complementation was assayed in solutions containing ^{SUMO}Sm-S1 and ^{SUMO}Lg-S2 and d-NSP10 added together in a ratio of 1:1:1 over a dilution series from 1×10^{-7} M to 48×10^{-12} M. As a control, we measured spontaneous NanoBiT complementation from ^{SUMO}Sm-S1 and ^{SUMO}Lg-S2 over that same concentration range but without d-NSP10 template (Supporting Fig. 4). Additional negative control experiments were carried out using ^{SUMO}Sm-S1 and ^{SUMO}Lg-S2 mixed with ssDNA template of the same length as d-NSP10 but with randomized sequence; luminescent readings from samples with the random oligo were indistinguishable from the “no template” control (Fig. 3A, “random”). We also attempted to measure NanoBiT reconstitution with a ssDNA template where the hybridization site for ^{SUMO}Lg-S2 was mutated to a poly A track; luminescence again matched no template control readings (Fig. 3A, ”d-NSP10 ΔS2”). Based on the encouraging results from these preliminary studies, we selected 25×10^{-9} M as the working concentrations of ^{SUMO}Sm-S1 and ^{SUMO}Lg-S2 bioconjugate sensors. This format, which is similar to conditions reported for other in vitro NanoBiT complementation assays (Supporting Table 1), conserved NanoBiT-steramer components while providing signal/background of 30–60 fold and a lower limit for complementary template detection of 2×10^{-9} M.

As shown in Fig. 3B, luminescence from reconstituted NanoBiT plotted as a function of increasing d-NSP10 template yielded a bellshaped curve. “Hook-effect” behavior is consistent with noncooperative tripartite interactions where one component of the assembly provides a scaffold to bring the remaining two components together [20,39]. Here, the nucleic acid template, d-NSP10, is the scaffolding element. Signal/background was highest when the three components were equimolar. To the right of the equivalence point, the excess d-NSP10 template favors formation of enzymatically in-active binary complexes: d-NSP10 hybridized with ^{SUMO}Sm-S1 only, or with ^{SUMO}Lg-S2 only.

We found that NanoBiT reconstitution remained durable with several “mutant” d-NSP10 templates (Fig. 3C). We first tested templates where the ^{SUMO}Lg-S2 site contained single or double nucleotide substitutions (see Table 1: d-NSP10 (A to C); d-NSP10 (C to A); d-NSP10 (AC swap)). We observed only modest changes in luminescence, <1.5-fold, compared to the positive control, d-NSP10, Fig. 3C (yellow). Tolerance toward base-pair mismatches is not unexpected for a linear hybridization involving oligos of this length [40,41]. In a related split enzyme system, using oligodeoxynucleotide-modified fragments of dihydrofolate reductase, split enzyme reassembly could be driven by hybridization to a ssDNA template carrying as many as five mismatches (Supporting Table 1) [21].

Next, we tested templates in which the hybridization sites of ^{SUMO}Sm-S1 and ^{SUMO}Lg-S2 were perfectly complementary but spaced farther apart by insertions of 2, 4, 6, or 8 deoxy thymidine nucleotides (Table 1. See d-NSP10$(TT)_n$). In samples containing the spacer templates d-NSP10$(TT)_1$, d-NSP10$(TT)_2$ and d-NSP10$(TT)_3$ we observed NanoBiT signal indistinguishable from samples mixed with the starting d-NSP10, Fig. 3C (pink). Only d-NSP10$(TT)_4$ stood out in this comparison, and interestingly, the NanoBiT luminescence was enhanced slightly, suggesting that there is room for further design optimization. In summary, these results indicate that there is tolerance toward single and double nucleotide substitutions in the nucleic acid target sequence and that there is flexibility in the distance separating the sites for hybridization.

With the modified NanoBiT complementation system working largely as intended on ssDNA, we turned our attention to the detection of target RNA. A synthetic SARS-CoV-2 NSP10 gene (460 bp) was cloned into the pGEM-3 vector and transcribed in vitro in the forward and reverse directions to generate sense (+) and anti-sense (−) NSP10 RNA transcripts. Samples containing ^{SUMO}Sm-S1, ^{SUMO}Lg-S2 and equivalent concentration (25×10^{-9} M) of the purified anti-sense transcript generated strong NanoBiT signal (Fig. 4). Luminescence output was on par with samples containing equivalent concentration of d-NSP10. A hook-effect in concentration–response plots was also apparent using this RNA template (Supporting Fig. 5). By contrast, NanoBiT reconstitution was not supported by samples containing the NSP10 sense transcript, which harbors segments identical to the oligonucleotides in ^{SUMO}Sm-S1 and ^{SUMO}Lg-S2. In summary, the split NanoBiT-steramer conjugates provide hybridization-driven luminescence detection of ssDNA and RNA.

3. Conclusions

Molecular tools to detect dilute nucleic acid have broad utility in clinical and non-clinical settings. Assay formats vary widely, from quantitative real time PCR and nanopore-based sequencing to less resource intensive technologies involving chromogenic dyes and gel-based read outs [42–44]. PCR remains the gold standard, however experience from the COVID-19 pandemic shows that dependence on a single assay type leads to logistical challenges when testing demand surges; thus, having a menu of assay options is important. Our focus is on integrating reporter enzymes into molecular assays as amplifiers of output signals to enhance sensitivity. In this study, we designed, prepared and validated a prototype split enzyme complementation assay driven by hybridization on ssDNA or RNA template. We attached monosterylated oligodeoxynucleotides (steramers) site-specifically to the

carboxy termini of NanoBiT enzyme fragments using the self-cleaving *Drosophila* hedgehog autoprocessing enzyme, DHhC. Direct 1:1 attachment of oligonucleotides to split enzyme fragments by a small molecule linker, rather than through a self-labeling biomacromolecule, increases the likelihood of productive protein fragment complementation. Replacing a self-labeling protein with small molecule linkers may be beneficial for split protein reconstitution on shorter nucleic acid templates, where a self-labeling protein might impose steric barriers to productive assembly.

Next generation nucleic acid biosensors of the general type described here will need to address limitations in mismatch discrimination as well as the hook-effect in concentration response plots. The weak mismatch discrimination observed here is not unexpected given the length of the probe oligos and the lack of hybridization constraints. We anticipate that substituting the linear oligo probes with hairpin oligos will increase the sequence specificity of template hybridization, as it does with molecular beacons [45,46]. With hairpin oligo probes, inter-molecular hybridization with template nucleic acid requires overcoming favorable intramolecular hybridization of the hairpin's stem regions. That thermodynamic constraint imposes greater demand for complementarity in hybridization, leading to enhanced specificity. Protein-steramer bioconjugation by DHhC proceeds unimpeded with hairpin oligos, making this an attractive enzymatic system to generate these biosensors [29]. The second challenge, posed by the hook-effect, threatens assay reliability through false negatives, where super stoichiometric nucleic acid template actually diminishes output signal. Engineering cooperativity into the NanoBiT/template assembly offers one potential solution [47]. For example, we are now pursuing NanoBiT hairpin probe oligos that not only hybridize to template with exquisite specificity, but also hybridize with each other following template hybridization, with the goal of yielding a 3-way junction (Supporting Fig. 6). Binding cooperativity in enzyme fragment complementation on template nucleic acid, if realized, is expected to avoid or at least lessen the hook effect phenomenon.

4. Afterword

As this work was underway, a biosensor for double stranded DNA with a conceptionally similar design to the present ssDNA/RNA biosensor system was reported wherein NanoBiT fragments were fused to a noncatalytic Cas9 protein (ncCas9) [20,48]. In that system, the ~160 kDa ncCas9 serves to (non-covalently) join LrgBiT and SmBiT to a short-guide RNA (sgRNA) in a manner similar to a self-labeling protein. The dynamic range (max signal/background) was similar to the 30–60 fold range reported here. Although the hook-effect was still observed, a practical advantage of using ncCas9 is that the sgRNA for DNA template recognition does not require chemical modification. The ncCas9 does, however, add considerable complexity and steric bulk to the NanoBiT bioconjugate sensor, which could conceivably complicate productive NanoBiT reconstitution [49]. A more serious limitation seems to be the intrinsic hybridization specificity of this ribonucleoprotein complex, restricting ncCas9-sgRNA-NanoBiT complementation to double stranded DNA targets that harbor a 5′-NGG-3′ PAM and its reverse complement 5′-CCN-3′ within 27–52 nucleotides of each other. Nonetheless, with an optimal template, the ncCas9/sgRNA/NanoBiT "LUNAS" method [20] showed impressive sensitivity and appeared amenable

to translation as a point-of-care diagnostic. Unfortunately, the specificity of LUNAS in discriminating mismatches in the DNA target was not reported.

Supplementary Material

Refer to Web version on PubMed Central for supplementary material.

Funding sources

We acknowledge generous support from the National Institute of Allergy and Infectious Diseases (Grant R03AI163907 to B.P.C.), and the National Institute of General Medical Sciences (Grant R35GM130207 to E.R.).

Appendix A.: Supplementary data

Vector construction, protein expression, steramer kinetic assays, chemical synthesis, NMR and MALDI-TOF. This material is available free of charge via the Internet at http://pubs.acs.org. Supplementary data to this article can be found online at https://doi.org/10.1016/j.bioorg.2024.108039.

Data availability

Data will be made available on request.

Abbreviations:

DHhC	Drosophila hedgehog C-terminal domain
SUMO	small ubiquitin modifier protein
MW	molecular weight
ssDNA	single stranded DNA
dsDNA	double stranded DNA
NSP10	non-structural protein 10
Ni-NTA	Nickel (2+)-Nitriloacetic acid
S1	steramer 1
S2	steramer 2
NSP	nonstructural protein
SEC	size exclusion chromatography

References

[1]. Ma C, et al. , The segment polarity gene hedgehog is required for progression of the morphogenetic furrow in the developing Drosophila eye, Cell 75 (5) (1993) 927–938. [PubMed: 8252628]

[2]. Skretas G, Wood DW, Regulation of protein activity with small-molecule-controlled inteins, Protein Sci. 14 (2) (2005) 523–532. [PubMed: 15632292]

[3]. Dagliyan O, et al. , Engineering extrinsic disorder to control protein activity in living cells, Science 354 (6318) (2016) 1441–1444. [PubMed: 27980211]

[4]. Blacklock KM, et al. , Computational design of a photocontrolled cytosine deaminase, J. Am. Chem. Soc 140 (1) (2018) 14–17. [PubMed: 29251923]

[5]. Szymanski W, et al. , Reversible photocontrol of biological systems by the incorporation of molecular photoswitches, Chem. Rev 113 (8) (2013) 6114–6178. [PubMed: 23614556]

[6]. Wu YI, et al. , Spatiotemporal control of small GTPases with light using the LOV domain, Methods Enzymol. 497 (2011) 393–407. [PubMed: 21601095]

[7]. Michnick SW, Exploring protein interactions by interaction-induced folding of proteins from complementary peptide fragments, Curr. Opin. Struct. Biol 11 (4) (2001) 472–477. [PubMed: 11495741]

[8]. Remy I, Michnick SW, Clonal selection and in vivo quantitation of protein interactions with protein-fragment complementation assays, Proc. Natl. Acad. Sci. USA 96 (10) (1999) 5394–5399. [PubMed: 10318894]

[9]. Johnsson N, Varshavsky A, Split ubiquitin as a sensor of protein interactions in vivo, Proc. Natl. Acad. Sci. USA 91 (22) (1994) 10340–10344. [PubMed: 7937952]

[10]. Rossi F, Charlton CA, Blau HM, Monitoring protein-protein interactions in intact eukaryotic cells by beta-galactosidase complementation, Proc. Natl. Acad. Sci. USA 94 (16) (1997) 8405–8410. [PubMed: 9237989]

[11]. Cabantous S, Waldo GS, In vivo and in vitro protein solubility assays using split GFP, Nat. Methods 3 (10) (2006) 845–854. [PubMed: 16990817]

[12]. Banaszynski LA, Wandless TJ, Conditional control of protein function, Chem. Biol 13 (1) (2006) 11–21. [PubMed: 16426967]

[13]. Fields S, Song O, A novel genetic system to detect protein-protein interactions, Nature 340 (6230) (1989) 245–246. [PubMed: 2547163]

[14]. Lan T, et al. , Development of luminescent biosensors for calprotectin, ACS Chem. Biol 19 (6) (2024) 1250–1259. [PubMed: 38843544]

[15]. Callahan BP, Stanger MJ, Belfort M, Protease activation of split green fluorescent protein, Chembiochem 11 (16) (2010) 2259–2263. [PubMed: 20945451]

[16]. Mootz HD, et al. , Conditional protein splicing: a new tool to control protein structure and function in vitro and in vivo, J. Am. Chem. Soc 125 (35) (2003) 10561–10569. [PubMed: 12940738]

[17]. Demidov VV, et al. , Fast complementation of split fluorescent protein triggered by DNA hybridization, Proc. Natl. Acad. Sci. USA 103 (7) (2006) 2052–2056. [PubMed: 16461889]

[18]. Furman JL, et al. , Toward a general approach for RNA-templated hierarchical assembly of split-proteins, J. Am. Chem. Soc 132 (33) (2010) 11692–11701. [PubMed: 20681585]

[19]. Zhou L, et al. , Tandem reassembly of split luciferase-DNA chimeras for bioluminescent detection of attomolar circulating microRNAs using a smartphone, Biosens. Bioelectron 173 (2021) 112824. [PubMed: 33229132]

[20]. van der Veer HJ, et al. , Glow-in-the-dark infectious disease diagnostics using CRISPR-Cas9-based split luciferase complementation, ACS Cent. Sci 9 (4) (2023) 657–667. [PubMed: 37122471]

[21]. Oltra NS, Bos J, Roelfes G, Control over enzymatic activity by DNA-directed split enzyme reassembly, Chembiochem 11 (16) (2010) 2255–2258. [PubMed: 20941727]

[22]. Dixon AS, et al. , NanoLuc complementation reporter optimized for accurate measurement of protein interactions in cells, ACS Chem. Biol 11 (2) (2016) 400–408.

[23]. Sekhon H, Loh SN, Engineering protein activity into off-the-shelf DNA devices, Cell Reports Methods 2 (4) (2022).

[24]. Chang D, et al. , Smartphone DNA or RNA sensing using semisynthetic luciferase-based logic device, ACS Sens. 5 (3) (2020) 807–813. [PubMed: 32124606]

[25]. Zhang X, et al. , Protein-nucleic acid conjugation with sterol linkers using hedgehog autoprocessing, Bioconjug. Chem 30 (11) (2019) 2799–2804. [PubMed: 31600061]

[26]. Porter JA, Young KE, Beachy PA, Cholesterol modification of hedgehog signaling proteins in animal development, Science 274 (5285) (1996) 255–259. [PubMed: 8824192]

[27]. Hall TM, et al. , Crystal structure of a Hedgehog autoprocessing domain: homology between Hedgehog and self-splicing proteins, Cell 91 (1) (1997) 85–97. [PubMed: 9335337]

[28]. Owen TS, et al. , Forster resonance energy transfer-based cholesterolysis assay identifies a novel hedgehog inhibitor, Anal. Biochem 488 (2015) 1–5. [PubMed: 26095399]

[29]. Zhang X, et al. , Enzymatic beacons for specific sensing of dilute nucleic acid, Chembiochem 23 (4) (2022) e202100594. [PubMed: 34890095]

[30]. Los GV, et al. , HaloTag: a novel protein labeling technology for cell imaging and protein analysis, ACS Chem. Biol 3 (6) (2008) 373–382. [PubMed: 18533659]

[31]. Lovendahl KN, Hayward AN, Gordon WR, Sequence-directed covalent protein-DNA linkages in a single step using HUH-tags, J. Am. Chem. Soc 139 (20) (2017) 7030–7035. [PubMed: 28481515]

[32]. Cooley R, et al. , Development of a cell-free split-luciferase biochemical assay as a tool for screening for inhibitors of challenging protein-protein interaction targets, Wellcome Open Res. 5 (2020) 20. [PubMed: 32587898]

[33]. Chretien AE, et al. , Extended linkers improve the detection of protein-protein interactions (PPIs) by dihydrofolate reductase protein-fragment complementation assay (DHFR PCA) in living cells, Mol. Cell Proteomics 17 (2) (2018) 373–383. [PubMed: 29203496]

[34]. Butt TR, et al. , Ubiquitin fusion augments the yield of cloned gene products in Escherichia coli, Proc. Natl. Acad. Sci. USA 86 (8) (1989) 2540–2544. [PubMed: 2539593]

[35]. Lin S, et al. , Crystal structure of SARS-CoV-2 nsp10/nsp16 2′-O-methylase and its implication on antiviral drug design, Signal Transduct. Target Ther 5 (1) (2020) 131. [PubMed: 32728018]

[36]. Krafcikova P, et al. , Structural analysis of the SARS-CoV-2 methyltransferase complex involved in RNA cap creation bound to sinefungin, Nat. Commun 11 (1) (2020) 3717. [PubMed: 32709887]

[37]. Zhou L, et al. , Programmable low-cost DNA-based platform for viral RNA detection, Sci. Adv 6 (39) (2020).

[38]. Tasakis RN, et al. , SARS-CoV-2 variant evolution in the United States: High accumulation of viral mutations over time likely through serial Founder Events and mutational bursts, PLoS One 16 (7) (2021) e0255169. [PubMed: 34297786]

[39]. Douglass EF Jr, et al. , A comprehensive mathematical model for three-body binding equilibria, J. Am. Chem. Soc 135 (16) (2013) 6092–6099. [PubMed: 23544844]

[40]. Aboul-ela F et al. , Base-base mismatches. Thermodynamics of double helix formation for dCA3XA3G + dCT3YT3G (X, Y = A,C,G,T), Nucleic Acids Res. 13(13) (1985) 4811–4824. [PubMed: 4022774]

[41]. Urakawa H, et al. , Optimization of single-base-pair mismatch discrimination in oligonucleotide microarrays, Appl. Environ. Microbiol 69 (5) (2003) 2848–2856. [PubMed: 12732557]

[42]. Mereuta L, et al. , A nanopore sensor for multiplexed detection of short polynucleotides based on length-variable, poly-arginine-conjugated peptide nucleic acids, Anal. Chem 94 (24) (2022) 8774–8782. [PubMed: 35666169]

[43]. Vogels CBF, et al. , Analytical sensitivity and efficiency comparisons of SARS-CoV-2 RT-qPCR primer-probe sets, Nat Microbiol 5 (10) (2020) 1299–1305. [PubMed: 32651556]

[44]. Li Z, et al. , Development and implementation of a simple and rapid extraction-free saliva SARS-CoV-2 RT-LAMP workflow for workplace surveillance, PLoS One 17 (5) (2022) e0268692. [PubMed: 35617204]

[45]. Tyagi S, Kramer FR, Molecular beacons: probes that fluoresce upon hybridization, Nat. Biotechnol 14 (3) (1996) 303–308. [PubMed: 9630890]

[46]. Hunt EA, Deo SK, Bioluminescent stem-loop probes for highly sensitive nucleic acid detection, Chem. Commun. (Camb.) 47 (33) (2011) 9393–9395. [PubMed: 21769413]

[47]. Liu S, et al. , Rational screening for cooperativity in small-molecule inducers of protein-protein associations, J. Am. Chem. Soc 145 (42) (2023) 23281–23291. [PubMed: 37816014]

[48]. Liu L, Wang Y, Schmitt DL, LUNAS: a rapid and sensitive nucleic acid detection assay using split nanoluc luciferase complementation, ACS Cent. Sci 9 (4) (2023) 593–596. [PubMed: 37122472]

[49]. Heath NG, et al. , Imaging unique DNA sequences in individual cells using a CRISPR-Cas9-based, split luciferase biosensor, Front. Genome Ed 4 (2022) 867390. [PubMed: 35403097]

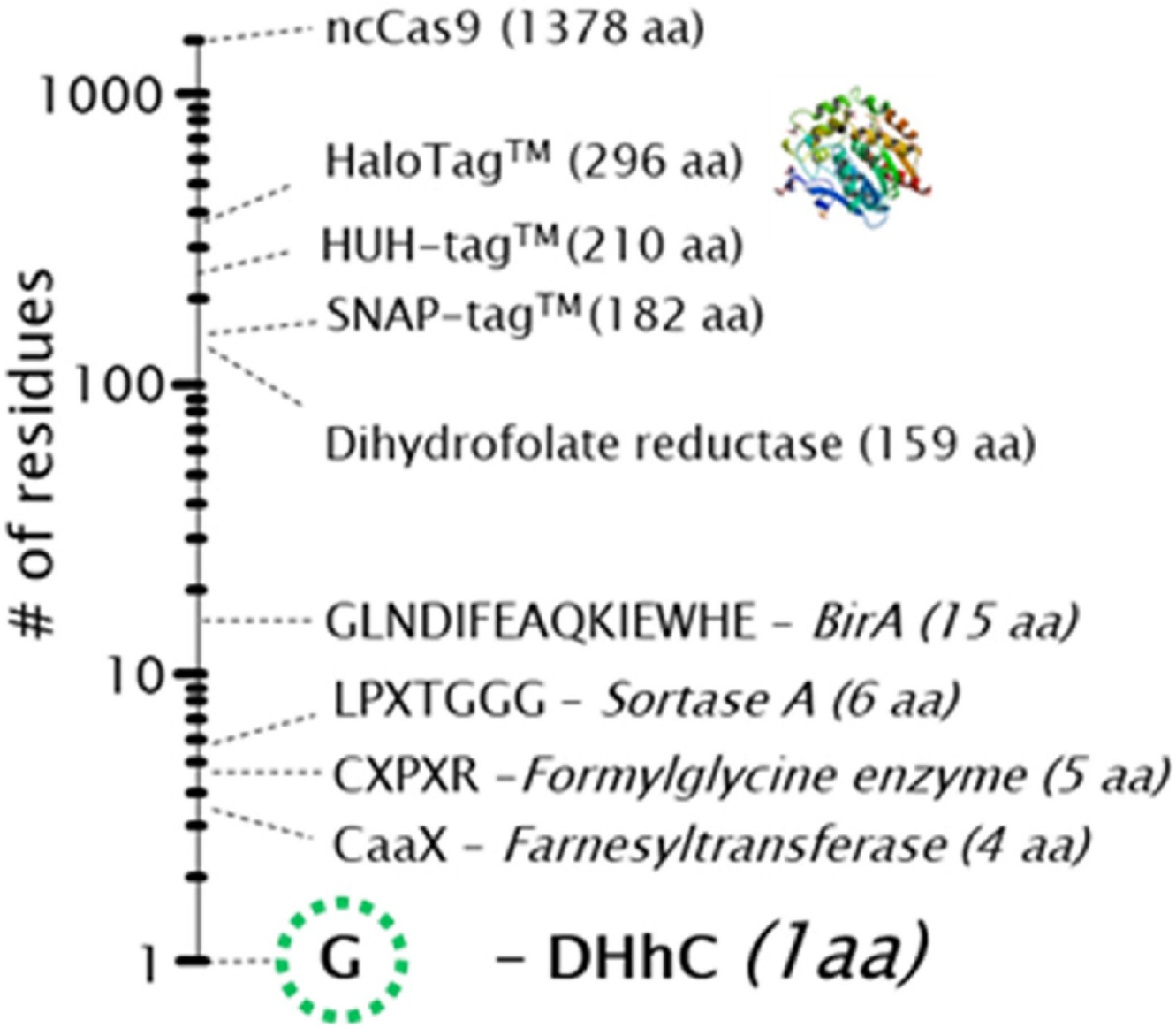

Fig. 1. Extraneous peptide or self-labeling domains left behind in the bioconjugate product cover a wide range.

Drosophila Hedgehog HhC (DHhC) catalyzed protein-nucleic acid conjugation, used in the present study, requires a small scar of a single glycine residue.

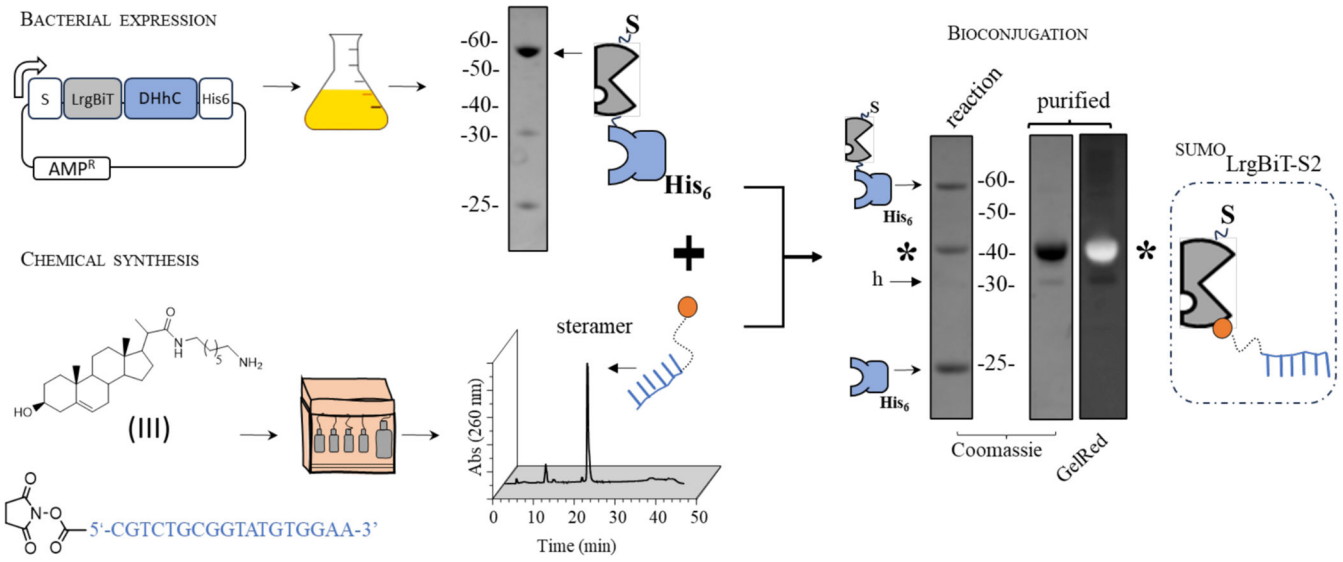

Fig. 2. Convergent chemi-enzymatic synthesis of NanoBiT fragment-oligonucleotide conjugates.

(Top, left) *E. coli* expression and purification of LrgBiT fusion with the bioconjugating domain, DHhC. Constructs contain an *N*-terminal SUMO (S) protein to enhance solubility and a C-terminal hexahistidine tag (His_6) for Ni-NTA chromatography. (Bottom, left) Steramer preparation. Monosterylation of oligodeoxynucleotides was carried out by amide coupling between (III, and orange circle) and NHS-ester modified oligodeoxynucleotides, followed by purification with reverse phase chromatography. (Side right) Bioconjugation. Precursor protein, ^{SUMO}LrgBiT-DHhC-His_6 is combined with steramer, leading to the displacement of DHhC-His_6 and covalent steramer attachment to ^{SUMO}LrgBiT, to yield ^{SUMO}LrgBiT-S2 (*). Competing side reaction where water replaces the steramer in the bioconjugation is minimal (h, product from hydrolysis). Bioconjugates were purified by agarose gel extraction, then concentrated by spin column. (For interpretation of the references to colour in this figure legend, the reader is referred to the web version of this article.)

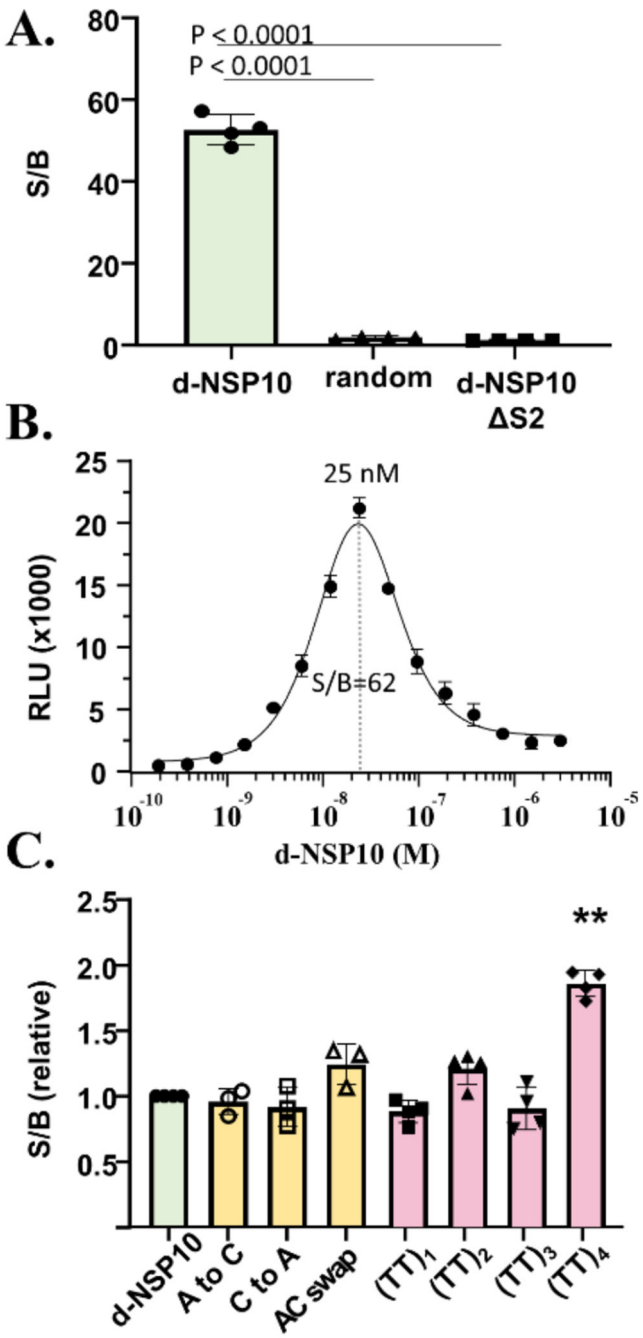

Fig. 3. NanoBiT fragment-steramer bioconjugates enable nucleic acid detection via protein fragment complementation.

A. Comparison of NanoBiT signal generated from samples containing the indicated ssDNA templates. Oligonucleotide templates, ^{SUMO}Sm-S1, ^{SUMO}Lg-S2 were (1:1:1), and added to 25×10^{-9} M, final. Statistical analysis: one-way ANOVA followed by T-test (GraphPad). **B**. Hook-effect apparent in concentration–response plot with increasing d-NSP10. **C**. Assessing NanoBiT reconstitution in the presence of nucleic acid template variants. Conditions same as (A). Only $(TT)_4$ showed a significant difference from control, d-NSP10. **, P < 0.0001.

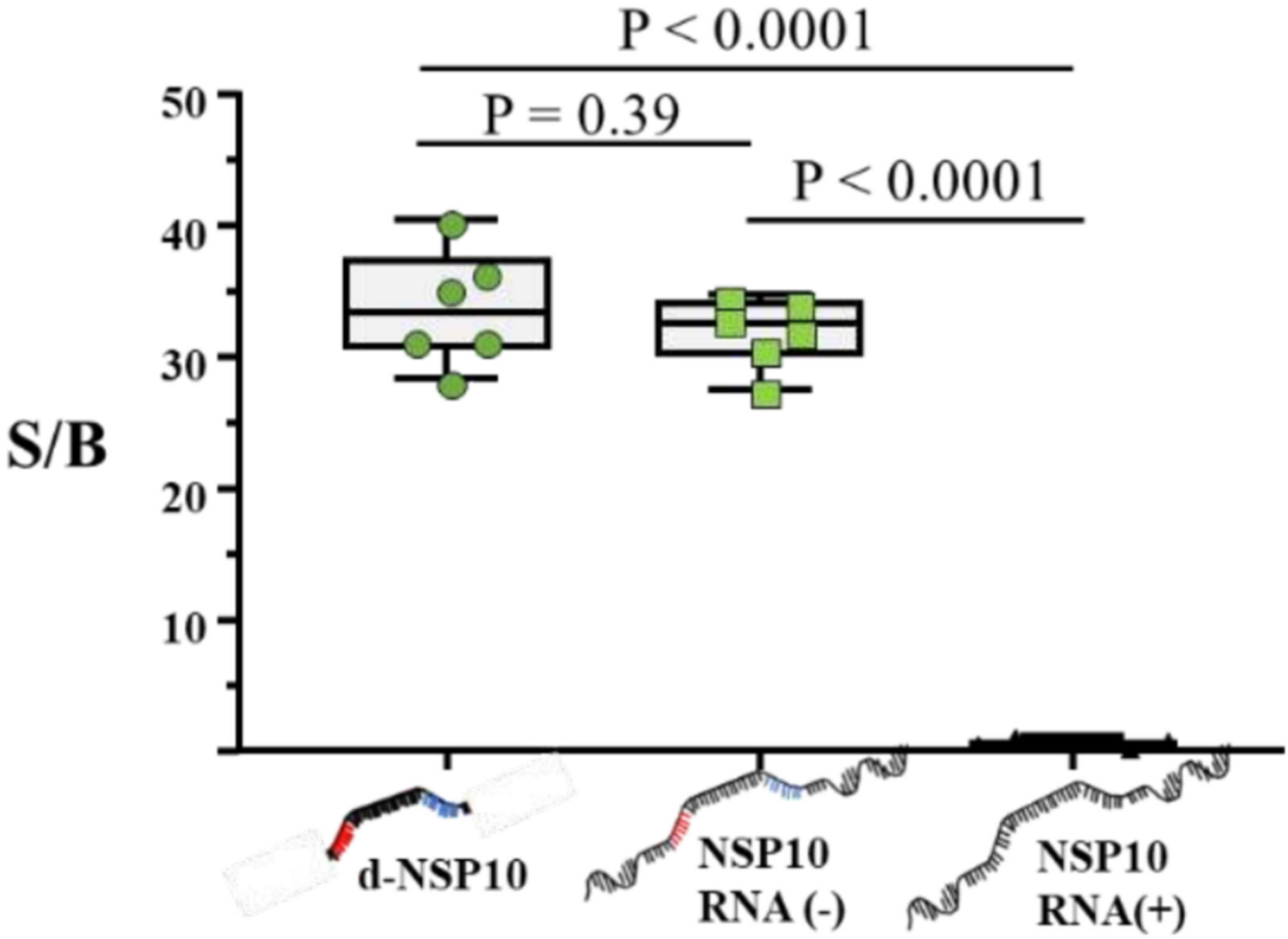

Fig. 4. NanoBiT reconstitution reports the presence of SARS-CoV-2 NSP-10 RNA.

In vitro transcribed anti-sense NSP10 RNA (squares) but not NSP10 sense RNA (triangles) triggers NanoBiT fragment assembly and enzymatic activity. Synthetic d-NSP10 served as a positive control (circles). Nucleic acid and NanoBiT components were added (1:1:1) to 25 × 10^{-9} M, final. Statistical analysis: one-way ANOVA followed by T-test (GraphPad).

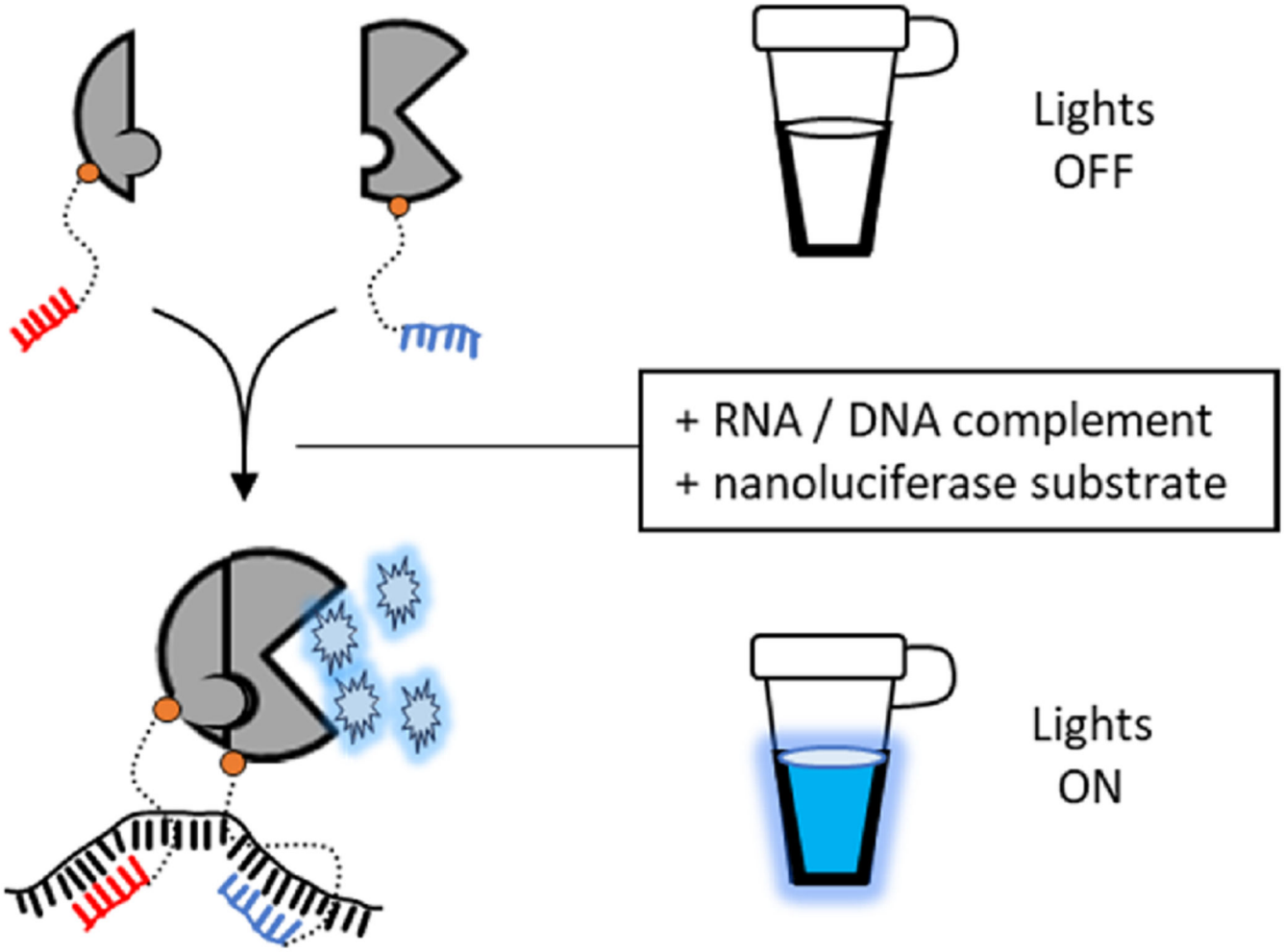

Scheme 1. Repurposing protein fragment complementation for DNA or RNA detection.
Split NanoBiT luciferase fragments with covalently attached oligonucleotides assemble into a functional light-emitting enzyme via template hybridization.

Table 1

Sequences of steramer 1 and 2 and nucleic acid targets evaluated here for potential hybridization-driven protein fragment complementation using the NanoBiT reporter enzyme.

Name	Sequence
Steramer-1 (S1)	sterol linker-5’-TTATGGCTGTAGTTGTGATC-3’
Steramer-2 (S2)	sterol linker-5’-CGTCTGCGGTATGTGGAA-3’
d-NSP10	5’-TTGATCACAACTACAGCCATAACCTTTCCACATACCGCAGACGGT-3’
random	5’-CTGATCCAGGAATACGTAAAAGATTATAATCGATATGACTGAGCG-3’
d-NSP10 ΔS2	5’-TTGATCACAACTACAGCCATAACCTAAAAAAAAAAAAAAAAAAT-3’
d-NSP10 (A to C)	5’-TTGATCACAACTACAGCCATAACCTTTCCACATCCCGCAGACGGT-3’
d-NSP10 (C to A)	5’-TTGATCACAACTACAGCCATAACCTTTCCACATAACGCAGACGGT-3’
d-NSP10 (AC swap)	5’-TTGATCACAACTACAGCCATAACCTTTCCACATCACGCAGACGGT-3’
d-NSP10$(TT)_n$	5’-TTGATCACAACTACAGCCATAAC$(TT)_n$CTTTCCACATACCGCAGACGGT-3’